analyzed for expression of CD25 and CD44. Biotinylated antibodies were visualized with streptavidin-RED670. Samples were analyzed by FACScan.
13. For the analysis of apoptosis, thymocytes were cultured for various times in 24-well flat-bottomed tissue culture plates at a density of 2×10^6 cells/ml in Iscove's modified Dulbecco's medium (10% fetal calf serum) and treated with apoptotic stimuli. Cells were harvested; stained with the 7-amino-actinomycin D (7-AAD), anti-CD4, and anti-CD8; and subjected to fluorescence-activated cell sorting (FACS) analysis. Apoptosis was confirmed with annexin V, propidium iodide, trypan blue, and 3,3'-dipropyloxacarbocyanine iodide.
14. D. Cournoyer and C. T. Caskey, *Annu. Rev. Immunol.* **11**, 297 (1993).
15. S. Huang, S. Apasov, M. Koshiba, M. Sitkovsky, *Blood* **90**, 1600 (1997).
16. M. Rincon *et al.*, *J. Exp. Med.* **188**, 1817 (1998).
17. D. A. Fruman *et al.*, *Science* **283**, 393 (1999); H. Suzuki *et al.*, *Science* **283**, 390 (1999).
18. Lymphocyte proliferation and cytokine production were determined as described (*21*). For mixed lymphocyte reactions, T cell–depleted, irradiated [20 grays (Gy)] splenic antigen-presenting cells from H-$2^{b/b}$ *PI3K*$\gamma^{+/-}$ and *PI3K*$\gamma^{-/-}$ mice were used as stimulators for allogeneic (H-$2^{d/d}$ and H-$2^{k/k}$) wild-type T cells.
19. Virus infections and hapten immunization were as follows. Mice were inoculated in one hind footpad with 2000 plaque-forming units (PFU) of LCMV-Armstrong (LCMV-Arm) in 30 μl of Hank's balanced salt solution. Footpad swelling was assessed daily with a spring-loaded caliper (*20*). LCMV-specific CTL activity of spleen cells was determined 10 days after infection by a ^{51}Cr-release assay with EL-4 target cells coated with the LCMV peptide NP118-126 or the nonspecific peptide AV (10^{-6} M). Percent specific ^{51}Cr release was calculated as [(experimental release – spontaneous release) × 100/(total release – spontaneous release)]. For hapten immunization, male mice were intraperitoneally immunized with 100 μg of the T cell–dependent haptenated protein NIP-OVA. NIP-specific IgG1 titers were determined by enzyme-linked immunosorbent assay (ELISA) on plates coated with NIP–bovine serum albumin.
20. W. P. Fung-Leung, T. M. Kündig, R. M. Zinkernagel, T. W. Mak, *J. Exp. Med.* **174**, 1425 (1991).
21. Y. Y. Kong *et al.*, *Nature* **397**, 315 (1999).
22. Q. Liu *et al.*, *Genes Dev.* **13**, 786 (1999); T. Sasaki, K. Hazeki, O. Hazeki, M. Ui, T. Katada, *Biochem. J.* **315**, 1035 (1996).
23. We thank M. Saunders, K. Bachmaier, Y. Kong, M. Crackover, E. Griffith, Q. Liu, V. Stambulic, L. Zhang, G. Duncan, C. Krawczyk, and D. Lacey for comments. T.S., J.I.-S., and J.M.P. are supported by the Medical Research Council and National Cancer Institute of Canada and by Amgen.

3 September 1999; accepted 16 December 1999

Roles of PLC-β2 and -β3 and PI3Kγ in Chemoattractant-Mediated Signal Transduction

Zhong Li,[1,2]* Huiping Jiang,[1]*† Wei Xie,[1]* Zuchuan Zhang,[1] Alan V. Smrcka,[1] Dianqing Wu[1,2]‡

The roles of phosphoinositide 3-kinase (PI3K) and phospholipase C (PLC) in chemoattractant-elicited responses were studied in mice lacking these key enzymes. PI3Kγ was required for chemoattractant-induced production of phosphatidylinositol 3,4,5-trisphosphate [PtdIns (3,4,5)P_3] and has an important role in chemoattractant-induced superoxide production and chemotaxis in mouse neutrophils and in production of T cell–independent antigen-specific antibodies composed of the immunoglobulin λ light chain (TI-Igλ_L). The study of the mice lacking PLC-β2 and -β3 revealed that the PLC pathways have an important role in chemoattractant-mediated production of superoxide and regulation of protein kinases, but not chemotaxis. The PLC pathways also appear to inhibit the chemotactic activity induced by certain chemoattractants and to suppress TI-Igλ_L production.

Chemoattractants have important roles in inflammatory reactions. Their receptors couple to the inhibitory heterotrimeric guanine nucleotide–binding proteins (G_i proteins) and elicit a wide range of responses in leukocytes (*1–3*). It is thought that two signaling pathways mediated by PLC (*4*) and PI3K (*5, 6*) are activated by chemoattractant receptors. To investigate the role of the PI3K-linked pathway in chemoattractant-mediated responses, we generated a mouse line that lacks PI3Kγ. A gene-targeting vector was constructed so that a green fluorescence protein (GFP) coding sequence was fused with the coding frame of PI3Kγ (Fig. 1A). Thus, the expression of GFP is under the control of the endogenous PI3Kγ promoter in the transgenic mice. The mice heterozygous and homozygous for the disrupted PI3Kγ genes were generated as described (*7*), and the genotypes were verified with Southern cDNA and Western blot analyses (Fig. 1A).

To determine the contribution of PI3Kγ to chemoattractant-induced PtdIns $(3,4,5)P_3$ production in mouse neutrophils, we compared formyl peptide *N*-formyl-Met-Leu-Phe (*f*MLP)–induced PtdIns $(3,4,5)P_3$ production in neutrophils from either wild-type or PI3Kγ-deficient mice (*8*). The neutrophils were prepared from the peritonea of mice treated with 2% casein (*9*). Although *f*MLP-elicited production of PtdIns $(3,4,5)P_3$ was clearly detected in the wild-type neutrophils, no production of PtdIns $(3,4,5)P_3$ was detected in response to *f*MLP in cells lacking PI3Kγ (Fig. 1B). This result indicates that PI3Kγ is the predominant PI3K isoform that mediates *f*MLP-induced PtdIns $(3,4,5)P_3$ production in mouse neutrophils.

The expression of PI3Kγ in mice was examined by detecting expression of GFP in the transgenic mice. GFP was detected in the spleen cells, bone marrow cells, and neutrophils isolated from mice homozygous for the disrupted PI3Kγ genes, but not those from wild-type mice (Fig. 1C). No GFP proteins were detected in other tested tissue samples of the PI3Kγ-deficient mice. These results suggest that the expression of PI3Kγ may be restricted to hematopoietic cells. GFP was detected with flow cytometry in over 90% of $Mac1^+$ cells in the peritoneum, and about 82% of $CD45R^+$ and 70% of $CD3^+$ cells from the spleens of transgenic mice also expressed GFP (*10*).

Chemoattractants can also activate PLC, leading to transient increases in intracellular Ca^{2+} concentrations. PLC-deficient mouse lines were generated to investigate the roles of PLC-β isoforms in leukocyte functions (Fig. 1D) (*11*). *f*MLP-induced inositol trisphosphate (IP_3) production and Ca^{2+} efflux were not detected in neutrophils lacking PLC-β2 and PLC-β3 (PLC-β2/-β3), while cells lacking only PLC-β2 also show clear reduction in IP_3 production and Ca^{2+} efflux (Fig. 1, E and F). Similar results were also observed with the other chemoattractants interleukin-8 (IL-8) and macrophage inflammatory protein (MIP)–1α (*10*). All these results support the conclusion that PLC-β2 and PLC-β3 are the sole PLC isoforms that are activated by chemoattractants in mouse neutrophils.

Chemoattractants induce various responses in leukocytes, one of which is chemotaxis. Neutrophils purified from casein-treated PLC-β2/-β3–null mice did not show differences from wild-type cells in *f*MLP-induced (Fig. 2A) or IL-8–induced (*10*) chemotactic activities. Thus, we conclude that the PLC pathway is not required for chemotaxis in neutrophils. Consistent with our previous report (*9*), PLC-β2/-β3–null neutrophils showed enhanced chemotactic activities in response to the CC chemokine MIP-1α (Fig. 2B). PI3Kγ deficiency impaired

[1]Department of Pharmacology, University of Rochester, Rochester, NY 14642, USA. [2]Department of Genetics and Developmental Biology, University of Connecticut Health Center, Farmington, CT 06030, USA.

*These authors contributed equally to this work.
†Present address: Department of Pharmacology, Boehringer Inglheim Pharmaceuticals, Inc., Ridgefield, CT 06877, USA.
‡To whom correspondence should be addressed. E-mail: dwu@neuron.uchc.edu

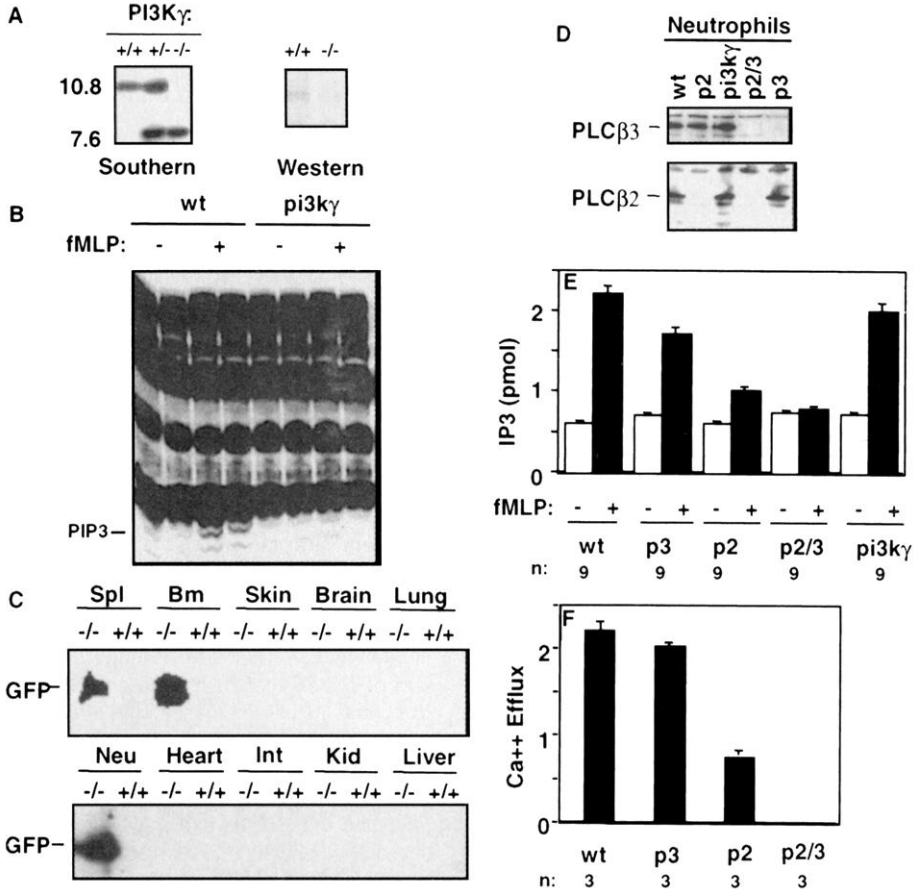

Fig. 1. Generation and characterization of the mouse lines that lack PI3Kγ, PLC-β2, and PLC-β3. (**A**) Southern cDNA and Western blot analyses. Mouse tail DNA was digested with Eco RI and hybridized with a probe from the PI3K gene outside the gene-targeting construct. Equal amounts of neutrophil extracts were analyzed by Western blot with an antibody to PI3Kγ. (**B**) *f*MLP-induced PtdIns (3,4,5)P_3 (PIP_3) production. The levels of PtdIns (3,4,5)P_3 were determined as described (*8*). wt, wild type. (**C**) Expression of GFP in tissue samples from a wild-type mouse (+/+) and a mouse homozygous for the disrupted PI3Kγ genes (−/−). Tissue extracts were analyzed by Western blot with an antibody to GFP. Tissue sample abbreviations are as follows: Spl, spleen; Bm, bone marrow; Neu, neutrophil; Int, intestine; Kid, kidney. (**D**) Western blot analysis of PLC-deficient mice. Neutrophil extracts from wt, PLC-β2 (p2)–null mice, PI3Kγ (pi3kγ)–null mice, PLC-β3 (p3)–null mice, and PLC-β2/-β3 (p2/3)–null mice were analyzed with antibodies to PLC-β2 (lower panel) or PLC-β3 (upper panel). (**E**) *f*MLP (1 μM)–induced production of IP_3. Neutrophils were treated with 1 μM *f*MLP for 45 s and IP_3 concentration was determined with a radioreceptor assay (NEN, Boston, MA). (**F**) *f*MLP-induced Ca^{2+} efflux. Neutrophils were labeled with fura-2/AM and treated with 1 μM *f*MLP. Excitation ratios of 340/380 nm were measured in a fluorimeter.

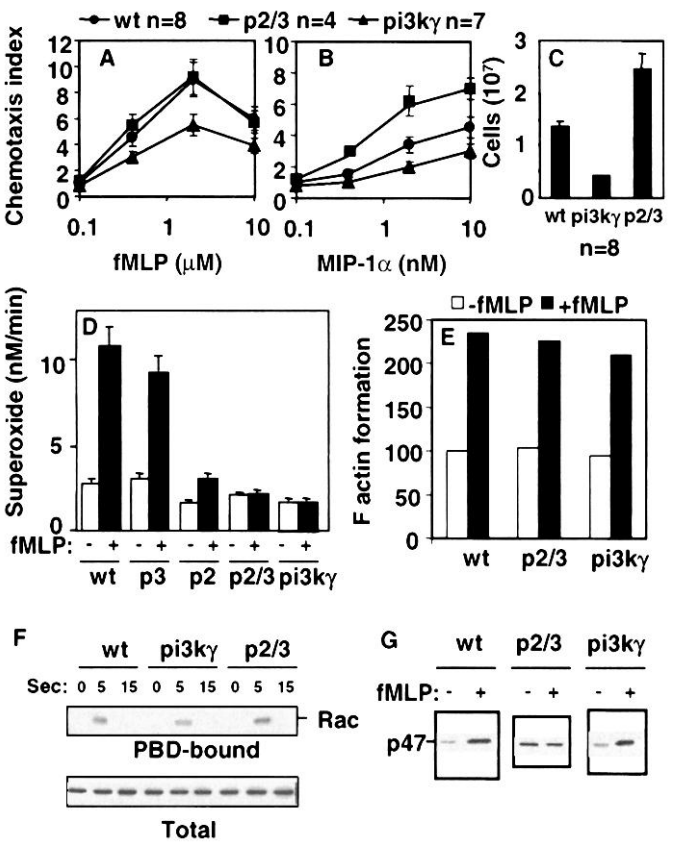

Fig. 2. Chemoattractant-induced responses in leukocytes. (**A** and **B**) Chemotaxis of purified casein-elicited neutrophils. *f*MLP-mediated (A) or MIP-1α–mediated (B) chemotaxis was determined in a 48-well modified Boyden chamber. The index represents the ratio of the number of migrated cells in the presence of ligand to those in the absence of ligand. (**C**) *E. coli*–induced peritonitis. *E. coli* (10^7) were injected into mice, and the number of cells in the peritonea was determined after 16 hours. Error bars represent SD. (**D**) Superoxide production determined in the presence or absence of 1 μM *f*MLP for 10 min at 37°C as described (*12*). The assay was performed in triplicate with six different sets of mice. Error bars represent SD. (**E**) F-actin formation. Neutrophils were treated with 1 μM *f*MLP for 45 s, and the levels of F-actin were determined in a flow cytometer after binding of rhodamime phalloidin. Experiments were repeated three times with three different sets of mice. The data shown are from a representative set. (**F**) Rac activation. The amount of GTP-bound Rac in the presence or absence of 1 μM *f*MLP was assayed by determining the levels of Rac that bound to the PBD of p21-activated protein kinase by Western blot with a Rac-specific antibody (*26*). Each experiment was repeated three times and used cells pooled from three to five mice. (**G**) Translocation of p47phox. Neutrophils (5×10^7) pooled from four mice were treated with 1 μM of *f*MLP for 45 s. Cytosolic and particulate fractions were prepared and analyzed with an antibody to p47phox. This experiment was performed twice. Abbreviations are the same as in Fig. 1.

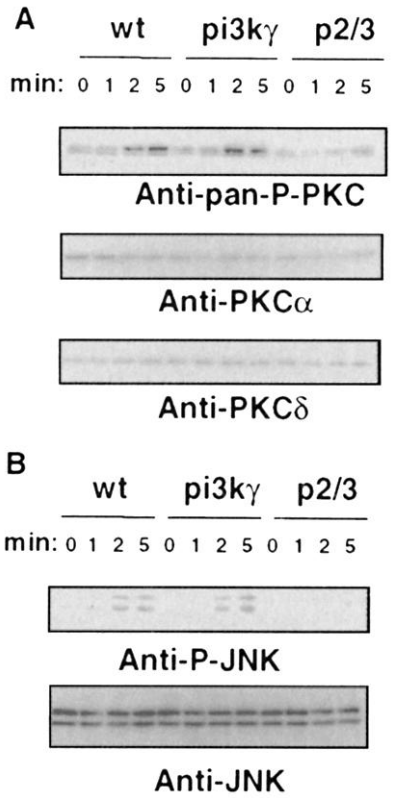

Fig. 3. Regulation of kinase activities. Casein-elicited neutrophils were treated with 1 μM of *f*MLP for varying times, and the same amount of cell extracts were subjected to Western analysis with an antibody that detects autophosphorylated PKC-α, -βI, -βII, -γ, and -δ (Anti-pan-P-PKC) and antibodies specific to PKC-α, and PKC-δ (**A**) and phospho-JNK and JNK (**B**). Representative experiments are shown. The experiments were repeated at least three times with three different sets of mice. Abbreviations are the same as in Fig. 1.

but did not eliminate the migration of neutrophils in response to *f*MLP or MIP-1α in an in vitro migration assay (Fig. 2, A and B). PI3Kγ deficiency also significantly impaired infiltration of neutrophils into the peritoneal cavity in *Escherichia coli*–induced peritonitis ($P < 0.01$), whereas PLC-β2/-β3–null mice showed enhanced infiltration of leukocytes (Fig. 2C). These results suggest that PI3Kγ has an important but not essential role in chemoattractant-induced chemotaxis of neutrophils.

Pharmacological studies suggest that PI3K may be required for chemoattractant-induced superoxide formation (*12*, *13*). Consistently, *f*MLP-induced superoxide production was insignificant in cells lacking PI3Kγ (Fig. 2D). PLC-β2/-β3–null cells also completely lost the ability to produce superoxide in response to *f*MLP (Fig. 2D). Thus, the PI3Kγ- and PLC-β–linked pathways are required for superoxide production. Regulation of Rac activity and p47phox translocation are two important steps in regulation of superoxide production, and both steps are influenced by various signaling pathways (*14*–*16*). PI3K has been implicated in regulation of Rac (*17*, *18*). However, neither PI3Kγ deficiency nor the PLC-β2/-β3 double deficiency had an effect on *f*MLP-induced activation of Rac in murine neutrophils (Fig. 2F). Thus, neither the PLC- nor the PI3K-linked pathway is required for activation of Rac. This conclusion is further supported by the lack of effect of these deficiencies on actin polymerization (Fig. 2E). Although *f*MLP-stimulated translocation of p47phox was observed in cells lacking PI3Kγ, the process did not occur in PLC-β2/-β3–null cells (Fig. 2G). These results indicate that the PLC-linked pathway rather than the PI3Kγ-linked pathway is required for p47phox translocation, and this may account for the failure to produce superoxide in response to *f*MLP in cells lacking PLC.

Protein kinase C (PKC) has been implicated in regulation of p47phox translocation (*19*). *f*MLP stimulates PKC activity, manifested as increases in autophosphorylation of PKC (*20*) (Fig. 3A). PLC deficiency blocked *f*MLP-induced autophosphorylation of PKC, but PI3Kγ deficiency did not (Fig. 3A). This result appears to contradict the finding that PKC activation requires the phosphorylation of the activation loop by a PtdIns $(3,4,5)P_3$–dependent mechanism (*21*). A possible explanation for this may be that the PKC molecules may already have been phosphorylated by basal PI3Kγ activity or by other PI3K isoforms.

Chemoattractant receptors activate mitogen-activated protein kinases (MAPKs), and PI3K has been implicated in mediating this activation. However, PI3Kγ deficiency did not obviously affect *f*MLP-induced activation of JNK (Fig. 3B) in mouse neutrophils. In contrast, PLC deficiency caused a reduction in chemoattractant-induced phosphorylation of JNK (Fig. 3B) and MAPK (*10*). Thus, the PLC pathway has a more important role than the PI3Kγ pathway in *f*MLP-induced JNK and MAPK activation in murine neutrophils. Our findings that PLC deficiencies impair JNK activation but not Rac activation suggest that Rac is not sufficient to activate JNK in mouse neutrophils.

PI3Kα regulates B cell development (*22*, *23*). We investigated whether PI3Kγ also influences B cell functions. Analyses with flow cytometry did not reveal differences between the wild-type and PI3Kγ-deficient mice in the pop-

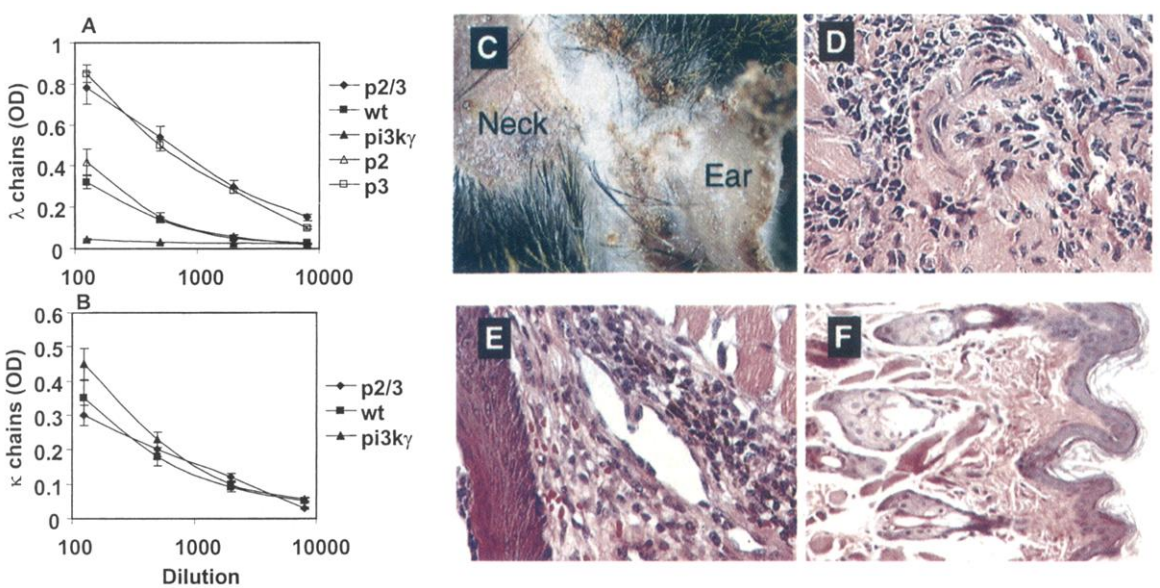

Fig. 4. Systemic phenotypes. (**A** and **B**) Production of TI-Igλ_L in mice. Mice were immunized with TI antigen NP-Ficoll, and the sera were collected 7 days after immunization (*27*). The amount of NP-specific λ chains (A) and κ chains (B) was determined by ELISA. The data presented are subtracted by the measurements of the corresponding pre-immune sera. In (A), $n = 18$ for p2/3, wt, and pi3kγ; $n = 6$ for p2 and p3. In (B), $n = 18$ for p2/3, wt, and pi3kγ. (**C** through **F**) Spontaneous skin ulcers in PLC-β3–deficient mice. A representative lesion area of a PLC-β3–deficient mouse is shown in (C). Histological sections of the tissue lesions (D) and (E) and normal tissue (F) are shown. Abbreviations are the same as in Fig. 1.

ulations of CD45R$^+$ cells in spleens or of CD45R$^+$ and CD43$^+$ cells in bone marrow (*10*). Unlike wild-type mice, however, mice lacking PI3Kγ produced few antibodies containing the λ light chain when immunized with T cell–independent (TI) antigen hydroxylnitrophenyl (NP)–Ficoll (Fig. 4A). By contrast, mice lacking both PLC-β2 and PLC-β3 consistently produced larger amount of TI antigen-specific antibodies composed of the immunoglobulin λ light chain (TI-Igλ$_L$) than did wild-type mice (Fig. 4A). It appears that the PLC pathway, in this case, opposes the PI3K pathway. Enhancement in TI-Igλ$_L$ production appeared to be primarily dependent on the PLC-β3 deficiency (Fig. 4A). Neither PLC nor PI3K deficiency affected the production of TI-Igκ (Fig. 4B) or of T cell–dependent (TD) antigen NP–chicken gamma globulin (NP-CCG)–specific antibodies composed of either λ or κ light chains (*10*). Together these data suggest that the production of TI-Igλ$_L$ may be subjected to regulation by G protein–mediated signaling pathways. Because no differences were detected between wild-type and PI3Kγ-deficient mice in the amount of total serum Igλ$_L$ and in the number of B cells carrying cell surface λ$_L$ (*10*), we think that PI3Kγ deficiency is more likely to affect antigen-dependent processes than early development of B cells.

Mice lacking PLC-β3 developed spontaneous multifocal skin ulcers usually starting at the age of 6 months or older (Fig. 4C). The lesions were localized mainly behind ears or on the neck, but sometimes also appeared on the face. Similar phenotypes were observed with mice lacking both PLC-β2 and PLC-β3. Histological examination of the lesion tissues revealed hyperinfiltration of leukocytes in the lesion tissues (Fig. 4, D and E). Most of the infiltrated leukocytes had morphological characteristics of macrophages and lymphocytes. No ulcerative lesions were observed in wild-type mice, mice heterozygous for the disrupted PLC-β3 genes, or other transgenic lines including PLC-β2– and PI3Kγ-null mice that were housed in the same rooms under the same conditions. This ulcerative phenotype is consistent with the idea that the PLC pathways act to inhibit some important responses mediated by chemoattractants.

In summary, this study with mouse lines deficient in two prominent chemoattractant-activated signaling pathways confirms that both PI3Kγ and PLC-β2/-β3 have important roles in chemoattractant-induced responses. The study also revealed roles for these proteins in leukocyte functions, including the involvement of PI3Kγ in the production of TI-Igλ$_L$ and the PLC pathway in down-modulation of chemotaxis and production of TI-Igλ$_L$ and in hyperinflammatory conditions.

References and Notes

1. M. Baggiolini, *Nature* **392**, 565 (1998).
2. B. A. Premack and T. J. Schall, *Nature Med.* **2**, 1174 (1996).
3. S. Jung and D. R. Littman, *Curr. Opin. Immunol.* **11**, 319 (1999).
4. D. Wu, G. J. LaRosa, M. I. Simon, *Science* **261**, 101 (1993).
5. B. Stoyanov *et al.*, *Science* **269**, 690 (1995).
6. L. R. Stephens *et al.*, *Cell* **89**, 105 (1997).
7. The PI3Kγ-deficient mouse line was generated by standard protocol (*11*). An 8-kb genomic DNA was isolated from a mouse 129sv genomic DNA library containing at least the first three exons of mouse PI3Kγ. A part of the first exon and entire second and third exons were replaced by the cDNA encoding GFP, which was fused in frame with the coding sequence of PI3Kγ. In addition, a neomycin–resistant gene expression unit was inserted behind GFP for selection of transfected embryonic stem (ES) cells. Three of the positive ES clones were used to produce chimeras. Mice heterozygous and homozygous for the disrupted PI3Kγ genes were produced by standard mating schemes.
8. The levels of PtdIns (3,4,5)P_3 were determined as described (*24*) with some modification. Mouse neutrophils (1×10^7) were labeled with [^{32}P]orthophosphate (1 mCi/ml) for 60 min at 37°C. After washing, cells were treated with 1 μM *f*MLP for 45 s. Lipid was extracted and analyzed on a 20 cm by 20 cm Silica Gel 60 thin-layer chromatography plate (EM Science, Gibbstown, NJ), as described in (*24*).
9. H. Jiang, Y. Kuang, M. I. Simon, D. Wu, *Proc. Natl. Acad. Sci. U.S.A.* **94**, 7971 (1997).
10. Z. Li *et al.*, data not shown.
11. W. Xie *et al.*, *Proc. Natl. Acad. Sci. U.S.A.* **96**, 10385 (1999).
12. C. J. Vlahos *et al.*, *J. Immunol.* **154**, 2413 (1995).
13. M. Thelen, M. P. Wymann, H. Langen, *Proc. Natl. Acad. Sci. U.S.A.* **91**, 4960 (1994).
14. U. G. Knaus, P. G. Heyworth, T. Evans, J. T. Curnutte, G. M. Bokoch, *Science* **254**, 1512 (1991).
15. A. Abo *et al.*, *Nature* **353**, 668 (1991).
16. G. M. Bokoch, *Curr. Opin. Cell Biol.* **6**, 212 (1994).
17. P. T. Hawkins *et al.*, *Biochem. Soc. Trans.* **25**, 1147 (1997).
18. J. Han *et al.*, *Science* **279**, 558 (1998).
19. J. W. Park and B. M. Babior, *J. Biol. Chem.* **267**, 19901 (1992).
20. L. M. Keranen, E. M. Dutil, A. C. Newton, *Curr. Biol.* **5**, 1394 (1995).
21. J. A. Le Good *et al.*, *Science* **281**, 2042 (1998).
22. D. A. Fruman *et al.*, *Science* **283**, 393 (1999).
23. H. Suzuki *et al.*, *Science* **283**, 390 (1999).
24. A. Ptasznik *et al.*, *J. Biol. Chem.* **271**, 25204 (1996).
25. V. Benard, B. P. Bohl, G. M. Bokoch, *J. Biol. Chem.* **274**, 13198 (1999).
26. The levels of guanosine triphosphate (GTP)–bound Rac were assayed by determining the amount of Rac associated with glutathione S-transferase–protein binding domain (GST-PBD) as described (*25*), with some modification. Murine neutrophils (1×10^7/50 μl) were treated with 4 μM *f*MLP for the durations indicated. The reaction was stopped by adding the same volume of the 2× lysis buffer [50 mM tris-HCl (pH 7.5), 10 mM $MgCl_2$, 200 mM NaCl, 2% NP-40, 10% glycerol, 2 mM phenylmethylsulfonyl fluoride, leupeptin (2 μg/ml), aprotinin (2 μg/ml), 2 mM orthovanadate, and 10 μg of GST-PBD]. The lysates were centrifuged for 3 min at 700*g*, and the supernatant was incubated with glutathione-Sepharose 4B beads for 1 hour at 4°C after addition of 200 μl of binding buffer [25 mM tris-HCl (pH 7.5), 1 mM dithiothreitol (DTT), 30 mM $MgCl_2$, 40 mM NaCl, and 0.5% Triton X-100]. The beads were washed three times with a washing buffer (the binding buffer with 1% Triton X-100) and washed one time with the binding buffer in the absence of Triton X-100. The beads were resuspended in SDS–polyacrylamide gel electrophoresis sample buffer and analyzed by Western blot with an antibody to Rac.
27. Mice (8 to 12 weeks old) were injected intraperitoneally with 10 μg of Alumn-precipitated NP32-Ficoll (TI) or NP22-CGG (TD). Sera were collected on day 7. Ten μl of serum was added to 100 μl of phosphate-buffered saline. Enzyme-linked immunosorbent assay (ELISA) was carried out in 96-well plates coated with NP30–bovine serum albumin with an ELISA kit from Zymed (South San Francisco, CA).

28. We thank M.-C. Dagher for antibody to p47phox, A. Pahxia for technical help, and A. Satterthwaite and O. Witte for critically reading this manuscript. Supported by grants to D.W. and A.V.S. from NIH and the American Heart Association.

17 September 1999; accepted 16 December 1999

Central Role for G Protein–Coupled Phosphoinositide 3-Kinase γ in Inflammation

Emilio Hirsch,[1]* Vladimir L. Katanaev,[2] Cecilia Garlanda,[3] Ornella Azzolino,[1] Luciano Pirola,[2] Lorenzo Silengo,[1] Silvano Sozzani,[3] Alberto Mantovani,[3,4] Fiorella Altruda,[1]† Matthias P. Wymann[2]*†

Phosphoinositide 3-kinase (PI3K) activity is crucial for leukocyte function, but the roles of the four receptor-activated isoforms are unclear. Mice lacking heterotrimeric guanine nucleotide-binding protein (G protein)–coupled PI3Kγ were viable and had fully differentiated neutrophils and macrophages. Chemoattractant-stimulated PI3Kγ$^{-/-}$ neutrophils did not produce phosphatidylinositol 3,4,5-trisphosphate, did not activate protein kinase B, and displayed impaired respiratory burst and motility. Peritoneal PI3Kγ-null macrophages showed a reduced migration toward a wide range of chemotactic stimuli and a severely defective accumulation in a septic peritonitis model. These results demonstrate that PI3Kγ is a crucial signaling molecule required for macrophage accumulation in inflammation.

Chemoattractant-mediated recruitment of leukocytes is a key step in the progress of acute and chronic inflammation. Chemokines and chemotactic peptides, such as *N*-formyl-Met-Leu-Phe (*f*MLP), C5a, and interleukin-8 (IL-8), bind to G protein–coupled re-